

CT Reconstruction using FBP with Sinusoidal Amendment for Metal Artefact Reduction

Julian J. Liu^{1,2}, Stephen R. Watt-Smith² and Stephen M. Smith¹

¹Oxford Centre for Functional Magnetic Resonance Imaging of the Brain,
University of Oxford, John Radcliffe Hospital, Oxford OX3 9DU, UK
liu@fmrib.ox.ac.uk

²Nuffield Department of Surgery, University of Oxford

Abstract. In this paper, a new method for metal artefact reduction in computed tomography is investigated, based on sinusoidal amendment. Each voxel in the scanned object corresponds to a sinusoidal curve in the projection data set. Some of the sinusoidal curves result from metal implant, which can be identified because the attenuation coefficient of the metal is much higher than that of human tissue, and therefore can be isolated from the projection, as well as reconstructed directly to provide the location of the metal implant. Then a highly accurate reconstruction image can be obtained using filtered back-projection because the original projection has been amended rather than interpolated. A real example is shown to demonstrate the method.

1 Introduction

Since the attenuation coefficient of metal is much higher than human tissue, a metal implant causes low signal to noise, beam hardening and scatter, which cause the projection data to be corrupted, and bring star-burst artefact and error to the reconstruction image. The filtered back-projection (FBP) method is the most widely method for reconstruction of the scanning data since it gives high computational efficiency whilst keeping good accuracy [1], star-burst artefacts have been reduced by substituting the data corresponding to the projection lines through metal objects with the data from a neighborhood [2] or synthetic data using linear or polynomial interpolation strategies [3], or by adjusting the wavelet decomposition coefficients [4]. These methods are very effective for removing streaking generated by metal implants, and do not increase computational amount significantly. However, these strategies inevitably cause some information loss and can still result in artefacts.

Iterative algorithms have been regarded as a potential method of providing high quality CT reconstruction images, especially for metal artefact reduction [5-8]. Using an iterative algorithm, the data affected by the metal implant, instead of being replaced, is ignored. Computational expense was the main problem preventing the iterative method from practical clinical application, and much effort has therefore been focused on this subject [9][10].

An alternative strategy to avoiding metal artefact is by using low attenuation material such as Titanium [11][12]. However, this is not ideal for clinical

application because the X-ray attenuation characteristics should not be the primary factor in material selection.

Currently, the standard reconstruction strategy in clinical practice is still filtered back projection with linear interpolation, which is reasonable for some general applications. However, in some situations such as planning a metal implant replacement operation and post-operation observation, knowing the exact structure of the tissues surrounding the metal implant is highly important. Using filtered back projection with linear interpolation or nearest neighbor interpolation, the reconstruction image in the area near the boundary of the metal implant is most likely to be distorted. It is true that the information is still sufficient if the affected scan data is ignored, but FBP does not allow such a gap, which must be interpolated. The iterative method steers away from the metallic affected data successfully, so that high quality images can be obtained, but the computational expense is still a big problem which keeps the method from becoming a practical option.

In this paper, a method is presented to isolate the correspondence of the metal implant from the projection, and reconstruct the amended projection and the correspondence of the metal implant separately, then synthesize these reconstructions to reach the final image. It has the potential to be developed into a new reconstruction algorithm, for example, directly based on the sinusoidal representation. The outline of this paper is as follows: In section 2, the sinusoidal description of CT is briefly introduced. Section 3 discusses the sinusoidal amendment and reconstruction from the point of view of practical implementation. The new method is demonstrated as well as further described with a real example in section 4. Discussions and conclusions are given in the final section.

2 The Sinusoidal Description

Radon's description was very meaningful in Physics. When traveling through an object, X-rays are attenuated so that when the X-rays reach the detectors, the information about the densities of the object along the path is included. Now another description of CT projection is studied from the point of view of mathematics and geometry, and the idea is to investigate the result from each voxel of the object in the projection.

The simplest situation, parallel projection, is studied in this paper, but it is straightforward to extend the method to other situations including fan beam, cone beam, and cone beam spiral.

Let $f(x, y)$ denote the distribution of a slice of an object, θ represent the rotation angle of the scanner, and the scan centre be (x_c, y_c) . Consider a voxel located at (x_1, y_1) , when θ increases from 0 to π , the projection of the voxel located at (x_1, y_1) is actually a trajectory of a sinusoidal curve, in other words, an equipotential sinusoidal curve on which the value is; the curve can be expressed as

$$t = \sqrt{(x_1 - x_c)^2 + (y_1 - y_c)^2} \sin(\arctg \frac{y_1 - y_c}{x_1 - x_c} + \theta) \quad (1)$$

where t denotes the locations of the detectors. Let $M(\theta, t, x_1, y_1)$ represent the projection of the voxel at (x_1, y_1) without consideration of other voxels, which is actually a subsection of the real projection, and can be described as

$$M(\theta, t, x_1, y_1) = \begin{cases} f(x_1, y_1) & \text{when equation (1) is satisfied} \\ 0 & \text{else} \end{cases} \quad (2)$$

The real projection from the scanner can be represented as the sum of $M(\theta, t, x, y)$ for each location of (x, y) , that is

$$P(\theta, t) = \sum_{x,y} M(\theta, t, x, y) \quad (3)$$

Equation (3) is a new description, or decomposition, of the X-ray projection, which is based on sinusoidal curves and the attenuation coefficients of each voxel of the object, in an additional frame. The number of the sinusoidal curves equals the number of the voxels of the object, as well as the number of attenuation coefficients. Further details of the sinusoidal description of CT were discussed in [13].

3 Sinusoidal Amendment and Reconstruction

Conventional methods detect the data set affected by the metal implant view by view and the edge cannot in general be precisely identified. In parallel beam projection, each voxel in the object creates a sinusoidal curve, and the value on this curve is the attenuation coefficient. Since the attenuation coefficient of metal is significantly higher than that of human tissue, in each view, the observed data from some detectors corresponding to the metal implant are, if not significantly greater than all of the other observed data in the view, at least significantly greater than other observed data in a neighborhood. The affected data set can be detected in two steps; the first is to determine a candidate data set which contains the affected data set as much as possible, then to identify the affected subset by fitting the sinusoidal curves with the candidate data set.

Discretely, let $P(i, j)$, $i = 1, 2, \dots, nd$; and $j = 1, 2, \dots, nv$, represent the projection, where nd and nv denote the number of the detectors and the views, respectively. Because of scattering, strong noise will occur when x-rays travel through metal material, which can cause the projection values at some points much greater or smaller than those in their neighborhood and affect the detection. This can be decreased by smoothing, and the smoothed data set is only used for detection of the affected data set.

Prior to the detection of the data set affected by metal implant, several definitions are introduced.

Let $P_s(i, j)$ denote the smoothed $P(i, j)$, $V_{im}(j) = \max_{1 \leq i \leq nd} (P_s(i, j))$, $V_{gm} = \max_{\substack{1 \leq i \leq nd \\ 1 \leq j \leq nv}} (P_s(i, j))$, and

$$P_{lm}(i, j) = P_s(i, j) - V_{im}(j) + V_{gm} \quad (4)$$

where $i = 1, 2, \dots, nd$; $j = 1, 2, \dots, nv$.

A data set with same size of $P_m(i, j)$ is generated as follows

$$T(a, i, j) = \begin{cases} 0 & \text{when } P_m(i, j) \leq (1-a)V_{gm} \\ P_m(i, j) - (1-a)V_{gm} & \text{when } P_m(i, j) > (1-a)V_{gm} \end{cases} \quad (5)$$

where a is a threshold parameter and $a \in [0,1]$.

A subset of $T(a)$ which is regarded as the candidate set of the affected data set is presented as

$$S_c(a) = \{T(a, i, j) : T(a, i, j) > 0, i = 1, 2, \dots, nd; j = 1, 2, \dots, nv\} \quad (6)$$

Let $W_s(a)$ denote the power (or cardinality) of $S_c(a)$, so $W(a) \in [0, nd \cdot nv]$, and $W_s(a)$ is a nondecreasing function of single variable a .

Initially, let $a = 0.1$, the data set $S_c(0.1)$ includes some of the correspondence of the metal implant which consists of a group of sinusoidal curves, but not all of the correspondences of the metal implant. To include as much as possible of the correspondence of the metal implant, whilst keeping them identifiable from the set of $T(a)$, a suitable value of a is highly important, since a smaller value of a will cause the results of identification insufficient while a bigger parameter will lead the results to be unidentifiable. However, a is a sensitive parameter which can be easily affected by many factors such as the energy of X-ray, the particular part of human body, the size, shape, position, and the material of the metal implant etc. The parameter a can be determined by introducing another parameter b which is not sensitive to the factors mentioned above.

$$a = \max \{x : 0.1 < x < 1, \frac{W(x)}{W(0.1)} \leq b\} \quad (7)$$

Since parameter a is controlled by parameter b , only parameter b need to be identified. The parameter b is obtainable statistically or experimentally and usually bounded between 1.2 and 10, which could be a monotonic increasing function of the distance between the metal implant and the scanning centre. A more detailed investigation for calculation of parameter b will be presented in near future, relevant for a large number of real cases.

After the parameter a has been determined, a set including most of the correspondence of the metal implant is generated by equation (6), based on which the correspondence of the metal implant can be identified.

The identification of the correspondence of the metal implant is to find the sinusoidal curves completely, or 99%, included in $S_c(a)$. It is not necessary to evaluate all of the sinusoidal curves corresponding to the locations where the object is; the searching area should be limited to be as small as possible if the metal implant is surely included. In fact, two views with $\pi/2$ difference in $T(0.1)$ can roughly provide the location of the metal implant, which plays a key role for the computing efficiency. As a result, a group of sinusoidal curves are identified, which is regarded as the correspondence of the metal implant and expressed as P_m .

Ideally, the attenuation coefficient distributed on these curves should be obtainable from reference material, and the projection can be amended by subtracting the correspondence of the metal implant.

$$P_a = P - CP_m \quad (8)$$

where P_a is the amended projection, and C denotes the attenuation coefficient of the metal. However, due to beam hardening and scattering, the coefficient is usually not a constant but a variable. Accordingly, in practice, equation (8) is modified as

$$P_a = P - (C - C_b)P_m \tag{9}$$

where C_b represents the changing of the attenuation coefficient caused by beam hardening and scattering, which is a function of the rotation angle and the locations of the detectors. The coefficient C_b can be determined by referring to the neighborhood.

The amended projection P_a is reconstructed using FBP and most of the artefacts caused by the metal implant can be removed successfully. When the correspondence of the metal implant P_m has been detected, the location of the metal implant has been revealed as well, although it can also be reconstructed using FBP. Both of the results are then synthesized to generate the final reconstruction image.

4 A Real Example

A real example is processed using the method discussed above for demonstration. The steps include detection of the candidate set containing most of the correspondence of the metal implant, detection of the correspondence of the metal implant based on the sinusoidal curves, amendment, reconstructions, and synthesis to obtain the final image.

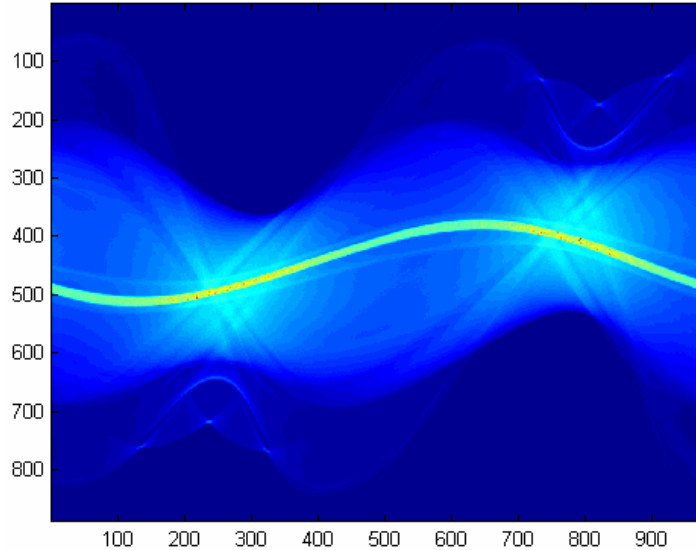


Fig. 1. The projection was collected from a clinical CT scanner.

The projection data in Fig. 1 was collected from a clinical CT scanner with the parameters of 140.0 KV, 40 mA, where the object was a leg of pork with a lead

nail inside the bone, which had been processed with scanner-specific pre-reconstruction preprocessing. The reconstruction image corresponding to Fig. 1 collected from the output of the scanner is shown in Fig. 2, where strong streaking takes place.

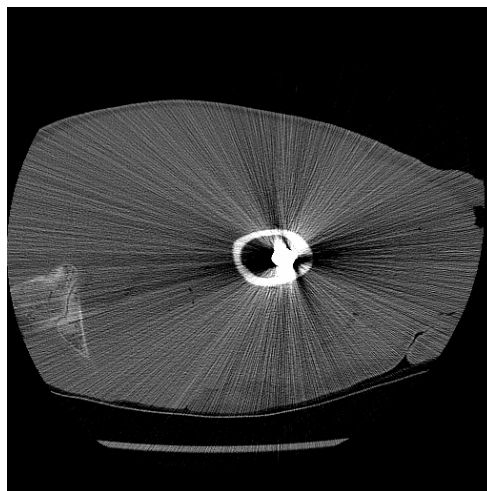


Fig. 2. The reconstruction of the projection in Fig. 1 created by the default scanner software (smaller field of view than in Fig. 6 due to clipping by the scanner software).

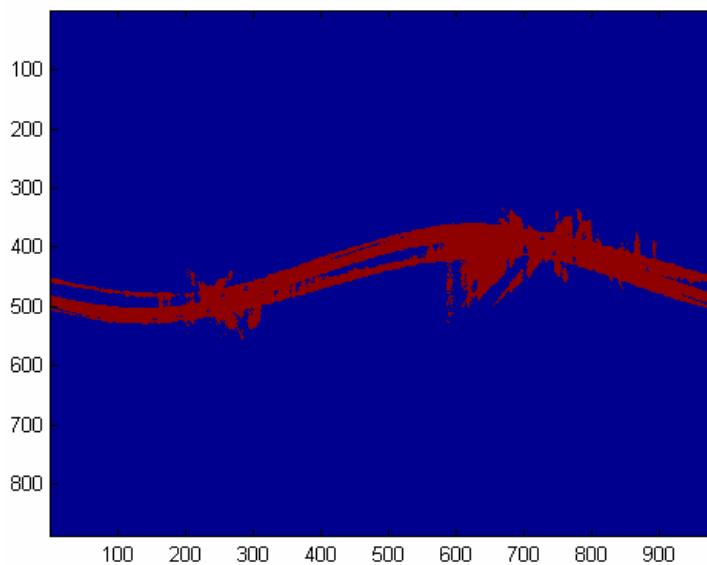


Fig. 3. The candidate set of the correspondence of the metal implant.

The parameter b in this section is determined as 3, and the parameter a is consequently calculated by equation (7) as 0.4. A set containing most of the

correspondence of the metal implant is generated by equation (6), denoted as $Sign [T(0.4)]$, as shown in Fig. 3.

The correspondence of the metal implant is identified and isolated from the projection, as shown in Fig. 4. The amended projection without the correspondence of the metal implant is shown Fig. 5.

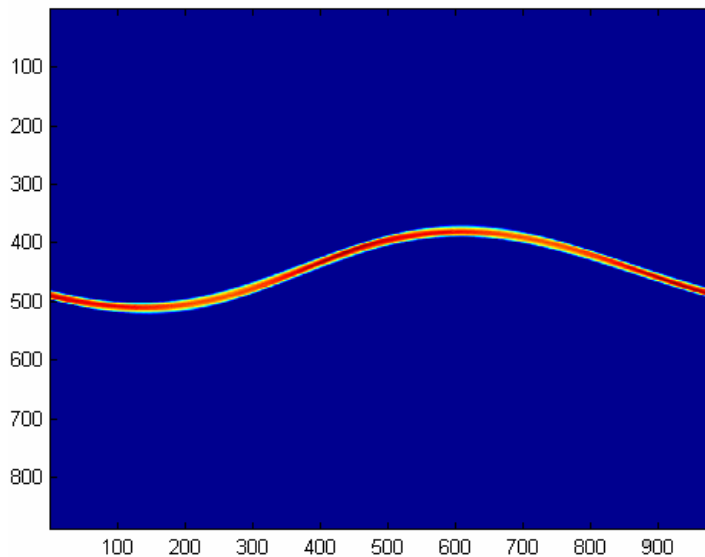


Fig. 4. The correspondence of the metal implant isolated from the projection.

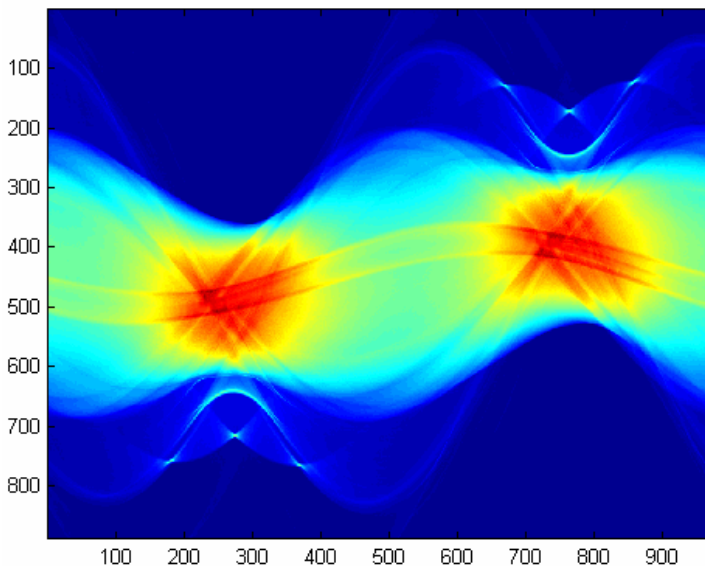


Fig. 5. The amended projection without the correspondence of the metal implant.

The final reconstruction image synthesized from the reconstruction of the correspondence of the metal implant in Fig. 4 and the amended projection in Fig. 5 using FBP is presented in Fig. 6.



Fig. 6. The final reconstruction image.

The whole reconstruction process for each slice costs about 6 minutes with a 2GH Pentium 4 using Matlab, which would be expected to be reduced to about 40 seconds if recoded using C++.

5 Discussions and Conclusions

The method presented in this study focuses on isolating the correspondence of the metal implant from the projection data set, then the amended projection can be reconstructed using FBP with much reduced metal artefact. The final reconstruction image is obtained by synthesizing the reconstructions of the amended projection and the metal correspondence. The amendment is automatically performed for a single piece of metal implant in this development, further studies will concentrate on extending the method to the case of multiple pieces of the metal implant such as planting the metal tooth root, for which it will be much more complex to amend the projection automatically. This method inherited the high computational efficiency of FBP, and can be clinically applied.

The conventional FBP just interpolates the affected data in projection, that reduces the streaking but causes other errors.

Iterative algorithms tend to successfully avoid using the affected data in the projection so they can reach high accuracy, but the calculation is complex and time consuming.

It is therefore predictable that the method of FBP with sinusoidal amendment will be applied practically in the near future.

Acknowledgment

The authors gratefully acknowledge that this study was supported by Action Research, and aided by the General Electric Company.

References

1. R.H. Bracewell and A.C. Riddle. *Inversion of fan beam scans in radio astronomy*. Astrophysics Journal, vol. 150, pp.427 - 434, 1967.
2. G. H. Glover and N. J. Pelc. *An algorithm for the reduction of metal clip artefacts in CT reconstructions*. Medical Physics, vol. 8, no. 6, pp.799-807, November-December, 1981.
3. W. A. Kalender, R. Hebel, and J. Ebersberger. *Reduction of CT artefacts caused by metallic implants*. Radiology, vol. 164, no. 2, pp.576-577, August 1987.
4. S. Zhao, D. D. Robertson, G. Wang, B. Whiting, and K. T. Bae. *X-ray CT metal artefact reduction using wavelets: an application for imaging total hip prostheses*. IEEE Transactions on Medical Imaging, vol. 19, no. 12, pp. 1238 ñ 1247, 2000.
5. J. Rockmore, A. Macovsky. *A maximum likelihood approach to emission image reconstruction from projections*. IEEE Trans. Nucl. Sci., vol. 23, no. 4, pp.1428-1432, 1976.
6. L. A. Shepp and Y. Vardi. *Maximum likelihood reconstruction for emission tomography*. IEEE Trans. Med. Imaging, vol. 1, no. 2, pp. 113-122, 1982.
7. J. Nuyts, B. De Man, P. Dupont, M. Defrise, P. Suetens, and L. Mortelmans. *Iterative reconstruction for helical CT: A simulation study*. Phys. Med. Biol., vol.43, pp. 729-737, 1998.
8. G. Wang, M. W. Vannier, and P. C. Cheng. *Iterative X-ray cone-beam tomography for metal artefact reduction and local region reconstruction*. Microscopy and Microanalysis, vol. 5, pp. 58-65, 1999
9. C. L. Byrne. *Convergent block-iterative algorithm for image reconstruction from inconsistent data*. IEEE Trans. Image Processing, vol. 6, no. 9, pp. 1296-1304, 1997.
10. C. L. Byrne. *Accelerating the EMMML algorithm and related iterative algorithms by rescaled block-iterative methods*. IEEE Trans. Image Processing, vol. 7, no. 1, pp. 100-109, 1998.
11. N. A. Ebraheim, R. Coombs, J. J. Rusin, and W. T. Jackson. *Reduction of postoperative CT artefacts of pelvic fractures by use of titanium implants*. Orthopedics, vol.13, pp.1357-1358, 1990.
12. C. Zannonia, M. Vicecontib, L. Pierottic and A. Cappelloa. *Analysis of titanium induced CT artefacts in the development of biomechanical finite element models*. Medical Engineering & Physics, vol. 20, no. 9, pp. 653-659, December 1998.
13. J. Liu, S. R. Watt-Smith and S. M. Smith. *A description of CT based on sinusoidal curves*. To appear in the Journal of X-ray Science & Technology.